Spin interactions and switching in vertically tunnel-coupled quantum dots

Guido Burkard,* Georg Seelig, and Daniel Loss†
Department of Physics and Astronomy, University of Basel, Klingelbergstrasse 82, CH-4056 Basel, Switzerland
(Received 7 October 1999)

We determine the spin-exchange coupling J between two electrons located in two vertically tunnel-coupled quantum dots, and its variation when magnetic (B) and electric (E) fields (both in-plane and perpendicular) are applied. We predict a strong decrease of J as the in-plane B field is increased, mainly due to orbital compression. Combined with the Zeeman splitting, this leads to a singlet-triplet crossing, which can be observed as a pronounced jump in the magnetization at in-plane fields of a few T, and perpendicular fields of the order of 10 T for typical self-assembled dots. We use harmonic potentials to model the confining of electrons, and calculate the exchange J using the Heitler-London and Hund-Mulliken techniques, including the long-range Coulomb interaction. With our results we provide experimental criteria for the distinction of singlet and triplet states, and therefore for microscopic spin measurements. In the case where dots of different sizes are coupled, we present a simple method to switch the spin coupling on and off with exponential sensitivity using an in-plane electric field. Switching the spin coupling is essential for quantum computation using electronic spins as qubits.

I. INTRODUCTION

Several methods to manipulate electronic spin in nanoscale semiconductor devices are being developed or are already available.[1] Perhaps even more challenging is the proposal to use the electron spin in quantum dots as the basic information carrier (the qubit) in a quantum computer.[2] The recently measured long decoherence times in semiconductor heterostructures[3] and quantum dots[4] are encouraging for the further research of solid-state quantum computation. Quantum logic gates between these qubits are effected by allowing the electrons to tunnel between two coupled quantum dots, thereby creating an effective spin-spin interaction. There is a large interest in quantum computation due to its potential of solving some classically intractable problems, such as factoring,[5] and speeding up the solution of other important problems, e.g., database search.[6] For the application of coupled quantum dots as a quantum gate, it is important that the coupling between the spins can be switched on and off via externally controlled parameters such as gate voltages and magnetic fields. In a recent publication,[7] we calculated the spin interaction for two laterally coupled and identical semiconductor quantum dots defined in a two-dimensional electron system (2DES) as a function of these external parameters, and found that the interaction J can be switched on and off with exponential sensitivity by changing the voltage of a gate located in between the coupled dots, or by applying a homogeneous magnetic field perpendicular to the 2DES. In this paper, we consider a different setup consisting of two *vertically* coupled quantum dots with magnetic as well as electric fields applied in the plane *and* perpendicular to the plane of the substrate (see Fig. 1). We also extend our previous analysis to coupled quantum dots of *different* sizes, which has important consequences for switching the spin interaction: When a small dot is coupled to a large one, the exchange coupling can be switched on and off with exponential sensitivity using an in-plane electric field $E_{\parallel}$.

Semiconductor quantum dots are small engineered structures which can host a single electron or a few electrons in a three-dimensionally confined region. Various techniques for manufacturing quantum dots, and methods for probing their physical properties (such as electronic spectra and conductance), are known.[8–10] In lithographically defined quantum dots, the confinement is obtained by electrical gating applied to a 2DES in a semiconductor heterostructure, e.g., in $Al_xGa_{1-x}As/GaAs$. In vertical dots, a columnar mesa structure is produced by etching a semiconductor heterostructure.[11] While laterally coupled quantum dots have been defined in 2DES's by tunable electric gates,[12–15] vertically coupled dots have been manufactured either by etching a mesa structure out of a triple-barrier heterostructure and subsequently placing an electrical side-gate around it,[16] or by using stacked double-layer self-assembled dots (SAD's).[17,18] In the mesa structure, the number of electrons per dot can be varied one by one starting from zero, whereas in SAD's the average number of electrons per dot in a sample with many dots can be controlled, even one electron per dot is experimentally feasible.[19]

Self-assembled quantum dots are manufactured in the so-

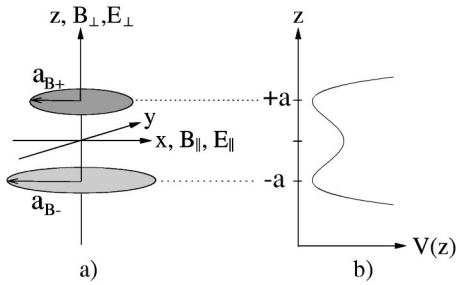

FIG. 1. (a) Sketch of the vertically coupled double quantum-dot system. The two dots may have different lateral diameters a_{B+} and a_{B-}. We consider magnetic and electric fields applied either in-plane ($B_{\parallel}$, $E_{\parallel}$) or perpendicularly ($B_{\perp}$, $E_{\perp}$). (b) The model potential for the vertical confinement is a double well, which is obtained by combining two harmonic wells at $z=\pm a$.

called Stranski-Krastanov growth mode, where a lattice-mismatched semiconducting material is epitaxially grown on a substrate, e.g., InAs on GaAs.[20] Minimization of the lattice mismatch strain occurs through the formation of small three-dimensional islands. Repeating the fabrication procedure described above, a second layer of quantum dots can be formed on top of the first one. Since the strain field of a dot in the first layer acts as a nucleus for the growth of a dot in the second layer, the quantum dots in the two layers are strongly spatially correlated.[21] Electrostatic coupling in vertical SADs has been investigated,[18] and it can be expected that the production of tunnel-coupled SADs will be possible in the near future.

In this paper, we concentrate on the magnetic properties (including in-plane fields $B_\parallel$) of pairs of quantum dots in which two electrons are vertically coupled via quantum tunneling and are subject to the full Coulomb interaction (see Fig. 1 for a sketch of the system under study). Coupled quantum dots in the absence of quantum tunneling (purely electrostatic interactions) were studied in Refs. 22–24. Electronic spectra and charge densities for two electrons in a system of vertically tunnel-coupled quantum dots at zero magnetic field were calculated in Ref. 25. Singlet-triplet crossings in the ground state of single[26] and coupled dots with two[27] to four[28,29] electrons in vertically coupled dots in the presence of a magnetic field perpendicular to the growth direction ($B_\parallel$ in Fig. 1) have been predicted.

In contrast to previous theoretical work on coupled dots,[22–29] the investigation presented here both takes into account quantum tunneling and includes *in-plane* magnetic fields ($B_\parallel$ in Fig. 1), leading to a much stronger suppression of the exchange energy than for $B_\perp$ (for very weakly confined dots, in-plane B fields can cause a singlet-triplet crossing, even in the absence of the Zeeman coupling). This result is in analogy with our earlier finding of a spin singlet-triplet crossing in laterally coupled identical dots as the perpendicular field is increased.[7] In addition to this, we investigate the influence of an electric field $E_\perp$ applied in the growth direction on low-energy electronic levels in vertically coupled quantum dots. From the electronic spectrum, we derive the equilibrium magnetization as a function of both the magnetic and electric fields (magnetization measurements for many-electron double quantum dots were reported in Ref. 30). As another important extension of earlier work, we consider a small dot which is tunnel coupled to a large dot. We find that this system represents an ideal candidate for a quantum gate, since the exchange interaction J can be switched simply by applying an in-plane electric field $E_\parallel$ (see Sec. V).

Our main interest is in the dynamics of the spins of the two electrons which are confined in the double dot. The spin dynamics can be described by an isotropic Heisenberg interaction

$$H_s = J\mathbf{S}_1 \cdot \mathbf{S}_2, \tag{1}$$

where the exchange energy J is the difference of the energies of the two-particle ground state, a spin singlet at zero magnetic field, and the lowest spin-triplet state. We shall calculate the exchange energy $J(\mathbf{B},\mathbf{E},a)$ of two vertically coupled quantum dots containing one electron each as a function of electric and magnetic fields ($\mathbf{E}$ and $\mathbf{B}$) and the interdot distance $2a$. We show that an in-plane magnetic field has a much stronger influence on the spin coupling than a perpendicular magnetic field. Moreover, we will discuss the influence of the dot size on J, and investigate systems containing two dots of different sizes. We will see that it is possible to suppress the spin-spin coupling exponentially by means of an in-plane magnetic field $B_\parallel$ for large dots (weak confinement) or, alternatively, with an in-plane electric field $E_\parallel$ if one of the dots is larger than the other. Furthermore we will point out differences and similarities in the field dependence of the tunnel splitting t found in a quantum mechanically coupled double-dot system containing only a single electron and the exchange energy J, a quantity due to two-particle correlations. Performing these calculations, we make use of methods known from molecular physics (Heitler-London and Hund-Mulliken technique), thus exploiting the analogy between quantum dots and atoms. Note again that besides being interesting in its own right, a quantum-dot ''hydrogen molecule,'' if experimentally controllable, could be used as a fundamental part of a solid-state quantum-computing device,[2,7] using the electronic spin as the qubit.

In our discussion of the vertically coupled double-dot system we proceed as follows. In Sec. II we introduce a model for a description of a vertical double-dot structure. Subsequently (Sec. III), we discuss vertically coupled quantum dots in perpendicular magnetic and electric fields. Section IV is devoted to the discussion of a double-dot structure in the presence of an in-plane magnetic field. In Sec. V we present a simple switching mechanism for the spin coupling involving an in-plane electric field. Finally, we discuss the implications of our result for two-spin and single-spin measurements in Sec. VI.

II. MODEL

The Hamiltonian which we use for the description of two vertically coupled quantum dots is

$$H = \sum_{i=1,2} h(\mathbf{r}_i, \mathbf{p}_i) + C,$$

$$h(\mathbf{r},\mathbf{p}) = \frac{1}{2m}\left(\mathbf{p} - \frac{e}{c}\mathbf{A}(\mathbf{r})\right)^2 + ezE + V_l(\mathbf{r}) + V_v(\mathbf{r}), \tag{2}$$

$$C = \frac{e^2}{\kappa|\mathbf{r}_1 - \mathbf{r}_2|},$$

where C is the Coulomb interaction and h the single-particle Hamiltonian. The dielectric constant κ and the effective mass m are material parameters. The potential V_l in h describes the lateral confinement, whereas V_v models the vertical double-well structure. For the lateral confinement we choose the parabolic potential

$$V_l(x,y) = \frac{m}{2}\omega_z^2 \begin{cases} \alpha_{0+}^2(x^2+y^2), & z>0 \\ \alpha_{0-}^2(x^2+y^2), & z<0, \end{cases} \tag{3}$$

where we have introduced the anisotropy parameters $\alpha_{0\pm}$ determining the strength of the vertical relative to the lateral confinement. Note that for dots of different size ($\alpha_{0+} \neq \alpha_{0-}$) the model potential [Eq. (3)] is not continuous at $z=0$. The lateral effective Bohr radii $a_{B\pm} = \sqrt{\hbar/(m\omega_z\alpha_{0\pm}}$ are

a measure for the lateral extension of the electron wave function in the dots. In experiments with electrically gated quantum dots in a two-dimensional electron system, it has been shown that the electronic spectrum is well described by a simple harmonic oscillator.[9,10] In the presence of a magnetic field $B_\perp$ perpendicular to the 2DES, the one-particle problem has Fock-Darwin states[32] as an exact solution. Furthermore, it has been shown experimentally[19] and theoretically[31] that a two-dimensional harmonic confinement potential is a reasonable approximation to the real confinement potential in a lens-shaped SAD. In describing the confinement V_v along the interdot axis, we have used a (locally harmonic) double-well potential of the form [see Fig. 1(b)]

$$V_v=\frac{m\omega_z^2}{8a^2}(z^2-a^2)^2, \tag{4}$$

which, in the limit of large interdot distance $a\gg a_B$, separates (for $z\approx\pm a$) into two harmonic wells (one for each dot) of frequency ω_z. Here a is half the distance between the centers of the dots and $a_B=\sqrt{\hbar/(m\omega_z)}$ is the vertical effective Bohr radius. For most vertically coupled dots, the vertical confinement is determined by the conduction-band offset between different semiconductor layers; therefore, in principle, a square-well potential would be a more accurate description of the real potential than the harmonic double well (note however, that the required conduction-band offsets are not always known exactly). There is no qualitative difference between the results presented below obtained with harmonic potentials and the corresponding results which we obtained using square-well potentials.[33]

It was shown in Refs. 7 and 34 that the spin-orbit contribution (due to the confinement) $H_{\rm so}=(\omega_z^2/2m_ec^2)\mathbf{S}\cdot\mathbf{L}$, with m_e being the bare electron mass, can be neglected in the relevant cases, e.g., $H_{\rm so}/\hbar\omega_z\sim10^{-7}$ for $\hbar\omega_z=30$ meV in GaAs.

The Zeeman splitting $H_Z=g\mu_B\Sigma_{i=1,2}\mathbf{B}\cdot\mathbf{S}_i$ is not included in the two-particle Hamiltonian [Eq. (2)], since in the absence of spin-orbit coupling one can treat the orbital problem separately and include the Zeeman interaction later (which we will do when we study the low-energy spectra and the magnetization). Here we have denoted the effective g factor by g and the Bohr magneton by μ_B.

III. PERPENDICULAR MAGNETIC FIELD $B_\perp$

We first study the vertically coupled double dot in a perpendicular magnetic field $B=B_\perp$ (cf. Fig. 1) which corresponds to the vector potential $\mathbf{A}(\mathbf{r})=\mathrm{B}(-y,x,0)/2$ in the symmetric gauge (for the time being, we set $E=0$).

The confining potentials for the two electrons are given in Eqs. (3) and (4). As a starting point for our calculations we consider the problem of an electron in a single quantum dot. The one-particle Hamiltonian by which we describe a single electron in the upper (lower) dot of the double-dot system is

$$h^0_{\pm a}(\mathbf{r})=\frac{1}{2m}\left(\mathbf{p}-\frac{e}{c}\mathbf{A}(\mathbf{r})\right)^2+\frac{m\omega_z^2}{2}[\alpha^2_{0\pm}(x^2+y^2)+(z\mp a)^2], \tag{5}$$

and has the ground-state Fock-Darwin[32] solution

$$\varphi_{\pm a}(x,y,z)=\left(\frac{m\omega_z}{\pi\hbar}\right)^{3/4}\sqrt{\alpha_\pm}\,e^{-m\omega_z[\alpha_\pm(x^2+y^2)+(z\mp a)^2]/2\hbar}, \tag{6}$$

corresponding to the ground-state energy $\epsilon_\pm=\hbar\omega_z(1+2\alpha_\pm)/2$. In Eq. (6) we have introduced $\alpha_\pm(\mathrm{B})=\sqrt{\alpha^2_{0\pm}+\omega_L(B)^2/\omega_z^2}=\sqrt{\alpha^2_{0\pm}+B^2/B_0^2}$, with $\omega_L(B)=eB/2mc$ the Larmor frequency and $B_0=2mc\omega_z/e$ the magnetic field for which $\omega_z=\omega_L$. The parameters $\alpha_\pm(B)$ describe the compression of the one-particle wave function perpendicular to the magnetic field. For finding the exchange energy J we make the Heitler-London ansatz, using the symmetric and antisymmetric two-particle wave-functions $|\Psi_\pm\rangle=(|12\rangle\pm|21\rangle)/\sqrt{2(1\pm S^2)}$, where we use the one-particle orbitals $\varphi_{-a}(\mathbf{r})=\langle\mathbf{r}|1\rangle$ and $\varphi_{+a}(\mathbf{r})=\langle\mathbf{r}|2\rangle$. Here $|ij\rangle=|i\rangle|j\rangle$ are two-particle product states, and $S=\int d^3r\,\varphi^*_{+a}(\mathbf{r})\varphi_{-a}(\mathbf{r})=\langle2|1\rangle$ denotes the overlap of the right and left orbitals. A nonvanishing overlap S implies that the electrons can tunnel between the dots. Using the two-particle orbitals $|\Psi_\pm\rangle$ we can calculate the singlet and triplet energy $\epsilon_{\rm s/t}=\langle\Psi_\pm|H|\Psi_\pm\rangle$, and therefore the exchange energy $J=\epsilon_t-\epsilon_s$. We rewrite the Hamiltonian, adding and subtracting the potential of the single upper (lower) dot for electron 1 (2) in H, as $H=h^0_{-a}(\mathbf{r}_1)+h^0_{+a}(\mathbf{r}_2)+W+C$, which is convenient because it contains the single-particle Hamiltonians h^0_{+a} and h^0_{-a} of which we know the exact solutions. The potential term is $W(\mathbf{r}_1,\mathbf{r}_2)=W_l(x_1,y_1,x_2,y_2)+W_v(z_1,z_2)$, where

$$W_l(x_1,y_1,x_2,y_2)=\sum_{i=1,2}V_l(x_i,y_i)-\frac{m\omega_z^2}{2}[\alpha^2_{0-}(x_1^2+y_1^2)+\alpha^2_{0+}(x_2^2+y_2^2)], \tag{7}$$

$$W_v(z_1,z_2)=\sum_{i=1,2}V_v(z_i)-\frac{m\omega_z^2}{2}[(z_1+a)^2+(z_2-a)^2]. \tag{8}$$

The formal expression for J is now

$$J=\frac{2S^2}{1-S^4}\left(\langle12|C+W|12\rangle-\frac{\mathrm{Re}\langle12|C+W|21\rangle}{S^2}\right). \tag{9}$$

Evaluating the matrix elements $\langle12|C+W|12\rangle$ and $\langle12|C+W|21\rangle$, we obtain

$$J=\frac{2S^2}{1-S^4}\hbar\omega_z\left\{c\sqrt{\mu}e^{2\mu d^2}[1-\mathrm{erf}(d\sqrt{2\mu})]-\frac{c}{\pi}\frac{\alpha_++\alpha_-}{\sqrt{1-(\alpha_++\alpha_--1)^2}}\arccos(\alpha_++\alpha_--1)+\frac{1}{4}(\alpha^2_{0+}-\alpha^2_{0-})\left(\frac{\alpha_+-\alpha_-}{\alpha_+\alpha_-}\right)[1-\mathrm{erf(d)}]+\frac{3}{4}(1+d^2)\right\}, \tag{10}$$

where $\mathrm{erf}(x)$ denotes the error function. We have introduced the dimensionless parameters $d=a/a_B$ for the interdot distance, and $c=\sqrt{\pi/2}(e^2/\kappa a_B)/\hbar\omega_z$ for the Coulomb interaction. Note that $\alpha_\pm$, $\mu=2\alpha_+\alpha_-/(\alpha_++\alpha_-)$, and the overlap

$$S=2\frac{\sqrt{\alpha_+\alpha_-}}{\alpha_++\alpha_-}\exp(-d^2), \tag{11}$$

depend on the magnetic field B. The first term in the square brackets in Eq. (10) is an approximate evaluation of the direct Coulomb integral $\langle 12|C|12\rangle$ for $d\gtrsim 0.7$ and for magnetic fields $B\lesssim B_0$.[35] The second term in Eq. (10) is the (exact) exchange Coulomb integral $\langle 12|C|21\rangle/S^2$, while the last two terms stem from the potential integrals, which were also evaluated exactly. If the two dots have the same size, the expression for the exchange energy [Eq. (10)] can be simplified considerably. We will first study the case of two dots of equal size, and later come back to the case of dots which differ in size.

Setting $\alpha_{0+}=\alpha_{0-}\equiv\alpha_0$ in Eq. (10), and using Eq. (11), we obtain

$$J=\frac{\hbar\omega_z}{\sinh(2d^2)}\left[c\sqrt{\alpha}e^{2\alpha d^2}[1-\mathrm{erf}(d\sqrt{2\alpha})]-\frac{c}{\pi}\frac{2\alpha}{\sqrt{1-(2\alpha-1)^2}}\arccos(2\alpha-1)+\frac{3}{4}(1+d^2)\right], \tag{12}$$

where $\alpha=\sqrt{\alpha_0^2+B^2/B_0^2}$. As before, the first term in Eq. (12) is the direct Coulomb term, while the second term (appearing with a negative sign) is the exchange Coulomb term. Finally, the potential term in this case equals $W=(3/4)(1+d^2)$, and is due to the vertical confinement only. For two dots of equal size neither the prefactor $2S^2/(1-S^4)$ nor the potential term depends on the magnetic field. Since the direct Coulomb term depends on $B_\perp$ only weakly, the field dependence of the exchange energy is mostly determined by the exchange Coulomb term.

Note that for obtaining the large-field asymptotics ($B\gtrsim B_0$), it would be necessary to include hybridized one-particle wave functions,[7] since in the magnetic field the level spacings between the one-particle ground states are shrinking and eventually become smaller than J, thus undermining the self-consistency of the one-orbital Heitler-London approximation. Increasing the interdot distance d (for a fixed confinement $\hbar\omega$), an exponential decrease of the exchange energy J is predicted by Eqs. (10) and (12). As mentioned, Eq. (10) is an approximation and should not be used for small interdot distances $d\lesssim 0.7$. There are also some limitations on the choice of the anisotropy parameters $\alpha_{0\pm}$. If we consider a system with much stronger vertical than lateral confinement (e.g., $\alpha_{0\pm}=1/10$), the exchange energy will become larger than the smallest excitation energy $\Delta\epsilon=\alpha_{0\pm}\hbar\omega_z$ in the single-dot spectrum. In that case we have to improve our Heitler-London approach by including hybridized single-dot orbitals.[7] If, on the other hand, the two dots are different in size, a double occupation of the larger dot is energetically favorable, and a Hund-Mulliken approach should be employed. In the Hund-Mulliken approximation, the Hilbert space for the spin singlet is enlarged by including two-particle states describing a double occupation of a quantum dot. Since only the singlet sector is enlarged it can be expected that we obtain a lower singlet energy ϵ_s than from the Heitler-London calculation (but the same triplet energy ϵ_t), and that therefore $J=\epsilon_t-\epsilon_s$ will be larger than the Heitler-London result [Eq. (10)].

We now apply the Hund-Mulliken approach to calculate the exchange energy of the double-dot system. We therefore introduce the orthonormalized one-particle wave functions $\Phi_{\pm a}=(\varphi_{\pm a}-g\varphi_{\mp a})/\sqrt{1-2Sg+g^2}$, where $g=(1-\sqrt{1-S^2})/S$. Using $\Phi_{\pm a}$, we generate four basis functions with respect to which we diagonalize the two-particle Hamiltonian H: States with double occupation, $\Psi^d_{\pm a}(\mathbf{r}_1,\mathbf{r}_2)=\Phi_{\pm a}(\mathbf{r}_1)\Phi_{\pm a}(\mathbf{r}_2)$, and states with single occupation, $\Psi^s_\pm(\mathbf{r}_1,\mathbf{r}_2)=[\Phi_{+a}(\mathbf{r}_1)\Phi_{-a}(\mathbf{r}_2)\pm\Phi_{-a}(\mathbf{r}_1)\Phi_{+a}(\mathbf{r}_2)]/\sqrt{2}$. Calculating the matrix elements of the Hamiltonian H in this orthonormal basis, we find

$$H=\begin{pmatrix} 2\epsilon+V_+ & -\sqrt{2}t_{H+} & -\sqrt{2}t_{H-} & 0\\ -\sqrt{2}t_{H+} & 2\epsilon_++U_+ & X & 0\\ -\sqrt{2}t_{H-} & X & 2\epsilon_-+U_- & 0\\ 0 & 0 & 0 & 2\epsilon+V_- \end{pmatrix}, \tag{13}$$

where

$$\epsilon_\pm=\langle\Phi_{\pm a}|h(z\mp a)|\Phi_{\pm a}\rangle,\quad \epsilon=\frac{1}{2}(\epsilon_++\epsilon_-), \tag{14}$$

$$t_{H\pm}=t-w_\pm=-\langle\Phi_{\pm a}|h|\Phi_{\mp a}\rangle-\frac{1}{\sqrt{2}}\langle\Psi^s_+|C|\Psi^d_{\pm a}\rangle, \tag{15}$$

$$V_\pm=\langle\Psi^s_\pm|C|\Psi^s_\pm\rangle,\quad U_\pm=\langle\Psi^d_{\pm a}|C|\Psi^d_{\pm a}\rangle, \tag{16}$$

$$X=\langle\Psi^d_{\pm a}|C|\Psi^d_{\mp a}\rangle. \tag{17}$$

The general form of the entries of the matrix [Eq. (13)] are given in Appendix A. The evaluation for perpendicular magnetic fields $B_\perp$ can be found in Appendix B. We do not display the eigenvalues of the matrix [Eq. (13)] here, since the expressions are lengthy. However, if the two dots have the same size ($\alpha_{0-}=\alpha_{0+}$), then the Hamiltonian considerably simplifies since $t_{H-}=t_{H+}\equiv t_H$, $\epsilon_+=\epsilon_-\equiv\epsilon$, and $U_+=U_-\equiv U$. In this case the eigenvalues are $\epsilon_{s\pm}=2\epsilon+U_H/2+V_+\pm\sqrt{U_H^2/4+4t_H^2}$ and $\epsilon_{s0}=2\epsilon+U_H-2X+V_+$ for the three singlets, and $\epsilon_t=2\epsilon+V_-$ for the triplet, where we have introduced the additional quantity $U_H=U-V_++X$. The exchange energy is the difference between the lowest singlet and the triplet state, $J=\epsilon_t-\epsilon_{s-}=V-U_H/2+\sqrt{U_H^2+16t_H^2}/2$, where we have used $V=V_--V_+$. The singlet energies ϵ_{s+} and ϵ_{s0} are separated from ϵ_t and ϵ_{s-} by a gap of order U_H and are therefore negligible for the study of low-energy properties. If only short-range Coulomb interactions are considered (which is usually done in the standard Hubbard approach) the exchange energy J reduces to $-U/2+\sqrt{U^2+16t^2}/2$, where t and U denote the hopping matrix element and on-site repulsion which are not renormalized by interaction. We call the quantities t_H and U_H the *extended* hopping matrix element and *extended* on-site repulsion, respectively, since they are renormalized by long-range

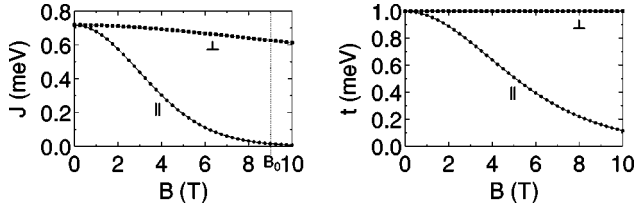

FIG. 2. Left graph: Exchange energy J as a function of the magnetic field B applied vertically to the xy plane ($B_\perp$, box symbols) and in-plane ($B_\parallel$, circle symbols), as calculated using the Hund-Mulliken method. Note that due to vertical orbital compression, the exchange coupling decreases much more strongly for an in-plane magnetic field. The parameters for this plot correspond to a system of two equal GaAs dots, each 17 nm high and 24 nm in diameter (vertical confinement energy $\hbar\omega_z = 16$ meV and anisotropy parameter $\alpha_0 = 1/2$). The dots are located at a center-to-center distance of $2a = 31$ nm ($d = 1.8$). The single-orbital approximation breaks down at about $B_0 \approx 9$ T, where it is expected that levels which are higher in the zero-field ($B = 0$) spectrum determine the exchange energy. Right graph: single-particle tunneling amplitude t vs magnetic field for the same system. Note that in contrast to the exchange coupling (a genuine two-particle quantity), t describes the tunneling of a *single* particle. Whereas J shows a weak dependence on the vertical magnetic field $B_\perp$, we note that $t(B_\perp)$ (box-shaped symbols) is constant.

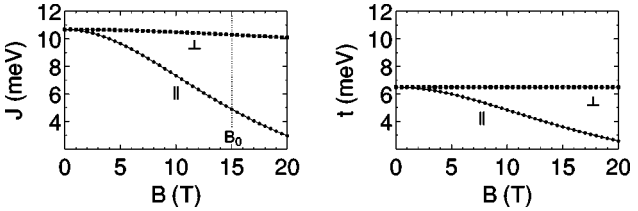

FIG. 3. Exchange energy J (left graph) and single-electron tunneling amplitude t (right graph) as a function of the applied magnetic field for two vertically coupled small (height 6 nm, width 12 nm) InAs ($m = 0.08 m_e$, $\kappa = 14.6$) quantum dots (e.g., self-assembled dots) in a center-to-center distance of 9 nm ($d = 1.5$). The box-shaped symbols correspond to the magnetic field $B_\perp$ applied in the z direction, and the circle symbols to the field $B_\parallel$ in the x direction. The plotted results were obtained using the Hund-Mulliken method, and are reliable up to a field $B_0 \approx 15$ T, where higher levels start to become important.

Coulomb interactions. If the Hubbard ratio t_H/U_H is $\lesssim 1$, we are in the Hubbard limit, where J approximately takes the form (cf. Ref. 7)

$$J = \frac{4t_H^2}{U_H} + V. \tag{18}$$

The first term in Eq. (18) has the form of the standard Hubbard model result, whereas the second term V is due to the long-range Coulomb interactions and accounts for the difference in Coulomb energy between the singlet and triplet states $\Psi_\pm^S$. We have evaluated our result for a GaAs ($m = 0.067 m_e$, $\kappa = 13.1$) system comprising two equal dots with vertical confinement energy $\hbar\omega_z = 16$ meV ($a_B = 17$ nm) and horizontal confinement energy $\alpha_0 \hbar\omega_z = 8$ meV in a distance $a = 31$ nm ($d = 1.8$). The result is plotted in Fig. 2 (left graph, box-shaped symbols). The exchange energy $J(B_\perp)$ as obtained from the Hund-Mulliken method for two coupled InAs SAD's ($m = 0.08 m_e$,[19] $\kappa = 14.6$, $\hbar\omega_z = 50$ meV, $\alpha_{0+} = \alpha_{0-} = 1/4$) is plotted in Fig. 3 (left graph, box symbols). Including the Zeeman splitting, we can now plot the low-energy spectrum as a function of the magnetic field; see Fig. 4 (left). Note that the spectrum clearly differs from the single-electron spectrum in the double dot (Fig. 4, right).

We now explain to what extent the Hund-Mulliken (HM) results (which we use for our quantitative evaluations of J) are more accurate than the results obtained from the Heitler-London (HL) method (which are more simple and which we used mostly for qualitative arguments). The Hund-Mulliken method improves on the Heitler-London method by taking into account double-electron occupancy of the quantum dots. The Hubbard ratio t_H/U_H can be considered a measure for the relative importance of double occupancy. Increasing the confinement $\hbar\omega_z$ at constant d (leading to potential wells that are deeper but closer together, since $a = d a_B = d\sqrt{\hbar/m\omega_z}$), we observe an increase in the discrepancy between J_{HM} and J_{HL} at zero magnetic field. Because the tunneling matrix element t is proportional to $\hbar\omega_z$ and the on-site repulsion U is proportional to the Coulomb energy $e^2/\kappa a_B \propto \sqrt{\hbar\omega_z}$, the Hubbard ratio t_H/U_H increases as $\sqrt{\hbar\omega_z}$ if the confinement is increased at constant distance; thus double occupancy becomes more important, explaining the increasing difference between J_{HM} and J_{HL}. Both increasing the interdot distance $2a$ and the confinement $\hbar\omega_z$ lead to a larger

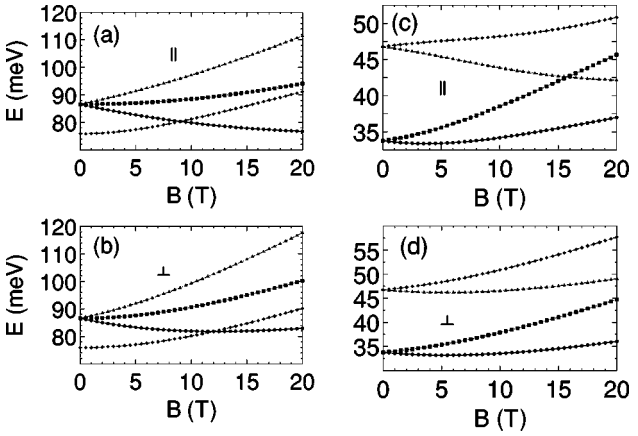

FIG. 4. Field dependence of the lowest four electronic levels for two vertically coupled InAs dots (parameters as in Fig. 3), including the Zeeman coupling with g factor $g_{\mathrm{InAs}} = -15$. Left graphs [(a) and (b)]: Spectrum for a two-electron system involving the Zeeman-split spin-triplet states (box, circle, and triangle symbols), and the spin-singlet (diamond symbols). The exchange energy J corresponds to the gap between the singlet and the middle ($m_z = 0$, box-shaped symbols) triplet energies. Under the influence of an in-plane field $\mathbf{B} \| x$ (a), the ground state changes from a singlet to a triplet at about 9 T, whereas in a perpendicular field $\mathbf{B} \perp x$ (b) the singlet-triplet crossing occurs at a higher field, about 12.5 T. Right graphs [(c) and (d)]; single-particle spectra, again plotted as a function of $B_\parallel$ (c) and $B_\perp$ (d). Note that single-particle and two-particle spectra are clearly distinguishable. In particular, there is no ground-state crossing for a single electron. The B field dependence of the spectrum of the large GaAs dots (cf. Fig. 2) is similar, with a much smaller Zeeman splitting ($g_{\mathrm{GaAs}} = -0.44$). The plots are reliable up to a field $B_0 \approx 15$ T, where higher levels start to become important.

value of $d=a/a_B$, and thus to a higher tunneling barrier. A strong decrease of the exchange energy J with increasing d is observed in both the result calculated according to the Heitler-London and Hund-Mulliken approaches.

We now turn to the dependence of the exchange energy J on an electric field $E_\perp$ applied in parallel to the magnetic field, i.e., perpendicular to the xy plane. Using the Heitler-London approach we find the result

$$J(B,E_\perp)=J(B,0)+\hbar\omega_z\frac{2S^2}{1-S^4}\frac{3}{2}\left(\frac{E_\perp}{E_0}\right)^2, \qquad (19)$$

where $E_0=m\omega_z^2/ea_B$. The growth of J is thus proportional to the square of the electric field $E_\perp$, if the field is not too large (see below). This result is supported by a Hund-Mulliken calculation, yielding the same field dependence at small electric fields, whereas if $eE_\perp a$ is larger than U_H, double occupancy must be taken into account. The electric field causes the exchange J at a constant magnetic field B to cross through zero from $J(E=0,B)<0$ to $J>0$. This effect is signalled by a change in the magnetization M; see Fig. 8.

In the presence of an electric field $E_\perp$, the ground-state energy of an electron in the dot at $z=\pm a$ is $\epsilon_\pm(E,B)=\hbar\omega_z[1+2\alpha_\pm(B)-(E/E_0)^2\pm 2dE/E_0]/2$. The shift of the ground-state energies for the upper (ϵ_+) and lower (ϵ_-) dot due to an electric field can be used to align the ground-state energy levels of two dots of different size (only for two dots of equal size, the energy levels are aligned at zero field). This is important because level alignment is necessary for coherent tunneling and thus for the existence of the two-particle singlet and triplet states. The parameter E_a denotes the electric field at which the one-particle ground states are aligned, $\epsilon_+(B,E_a)=\epsilon_-(B,E_a)$ (for dots of equal size, $E_a=0$). Investigating the dependence of J on $E_\perp$, one has to be aware of the fact that coherent tunneling is suppressed as the electric field is increased, since the single-particle levels are detuned (note, however, that the suppression is not exponential). This level detuning limits the range of application of Eq. (19), which is only valid for small level misalignment, $2e(E_\perp-E_a)a<J(0,0)$, where $J(0,0)$ is the exchange at zero field. Assuming gates at 20 nm below the lower and at 20 nm above the upper dot in the system discussed above ($2a\approx 31$ nm, $\hbar\omega_z=16$ meV, and $\alpha_0=1/2$), we find that $2aE_\perp e=J(0,0)\approx 0.7$ meV at a gate voltage of about $U\approx 1.6$ mV. A further condition for the validity of Eq. (19) is $J(E_\perp)<\hbar\omega_z\alpha_{0-}$, ($\alpha_{0-}\leqslant\alpha_{0+}$). If this condition is not satisfied, we have to use hybridized single-particle orbitals. For the parameters mentioned above, we find $J(E_\perp)=\hbar\omega_z\alpha_{0-}=8$ meV at a gate voltage $U\approx 270$ mV; therefore, this condition is automatically fulfilled if $2eE_\perp a<J(0,0)$. The numbers used here are arbitrary but quite representative, as typical exchange energies are on the order of a few meV and interdot distances usually range from a few nm to a few tens of nm.

In the case where one of the coupled quantum dots is larger than the other, there is a peculiar nonmonotonic behavior when a perpendicular field $B_\perp$ is applied at $E=0$, see Fig. 5. The wave-function compression due to the applied magnetic field has the effect of decreasing the size difference of the two dots, thus making the overlap [Eq. (11)] larger. This growth of the overlap saturates when the electron orbit in the larger dot has shrunk approximately to the size of the orbital of the smaller dot, which happens at roughly $B_{0+}=2mc\omega_z\alpha_{0+}/e$ (assuming that $\alpha_{0+}\geqslant\alpha_{0-}$).

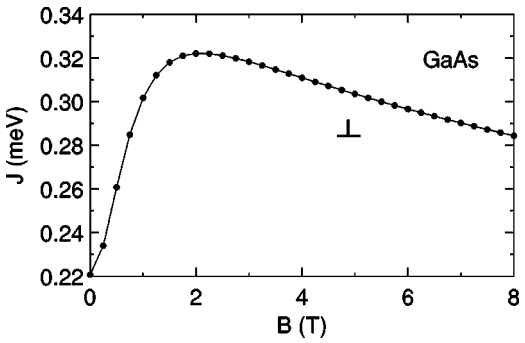

FIG. 5. Exchange energy J as a function of the perpendicular magnetic field $B_\parallel$ for two vertically coupled GaAs quantum dots of different sizes (both 25 nm high, the upper dot is 50 nm in diameter, and the lower dot is 100 nm in diameter; $B_{0+}\approx 2$ T and $d=1.5$). Here J is obtained using the Heitler-London method [Eq. (10)]. The nonmonotonic behavior is due to the increase in the overlap [Eq. (11)], when the orbitals are magnetically compressed, and therefore the size difference becomes smaller.

IV. IN-PLANE MAGNETIC FIELD $B_\parallel$

In this section we consider two dots of equal size in a magnetic field $B_\parallel$ which is applied along the x axis, i.e., *in plane* (see Fig. 1). Since the two dots have the same size, the lateral confining potential [Eq. (3)] reduces to $V(x,y)=m\omega_z^2\alpha_0^2(x^2+y^2)/2$, where the parameter α_0 describes the ratio between the lateral and the vertical confinement energy. The vertical double-dot structure is modeled using the potential [Eq. (4)]. The single-dot Hamiltonian is given by Eq. (5), with the vector potential $\mathbf{A}(\mathbf{r})=B(0,-z,y)/2$. The situation for an in-plane field is a bit more complicated than for a perpendicular field, because the planar and vertical motion do not separate. In order to find the ground-state wave function of the one-particle Hamiltonian $h^0_{\pm a}$, we have applied the variational method (cf. Appendix D), with the result

$$\varphi_{\pm a}(\mathbf{r})=\left(\frac{m\omega_z}{\pi\hbar}\right)^{3/4}(\alpha_0\alpha\beta)^{1/4}\exp\left[-\frac{m\omega_z}{2\hbar}(\alpha_0x^2+\alpha y^2+\beta(z\mp a)^2)\pm i\frac{ya}{2l_B^2}\right]. \qquad (20)$$

Note that this is not the exact single-dot ground state, except for spherical dots ($\alpha_0=1$). We have introduced the parameters $\alpha(B)=\sqrt{\alpha_0^2+(B/B_0)^2}$ and $\beta(B)=\sqrt{1+(B/B_0)^2}$, describing the wave-function compression in the y and z directions, respectively. The phase factor involving the magnetic length $l_B=\sqrt{\hbar c/eB}$ is due to the gauge transformation $\mathbf{A}_{\pm a}=B(0,-[z\mp a],y)/2\rightarrow\mathbf{A}=B(0,-z,y)/2$. The one-particle ground-state energy amounts to $\epsilon_0=\hbar\omega_z(\alpha_0+\alpha+\beta)/2$. From $\varphi_{\pm a}$ we construct symmetric and antisymmetric two-particle wave functions $\Psi_\pm$, exactly as for $\mathbf{B}\|z$. Care has to be taken calculating the exchange energy J; Eq. (9) has to be

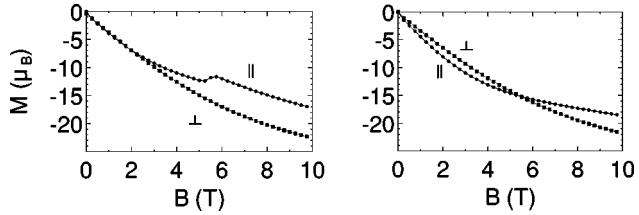

FIG. 6. Magnetization M (in units of Bohr magnetons) as a function of the B field for vertically coupled large GaAs ($g=-0.44$) quantum dots (parameters as in Fig. 2) containing two electrons (left graph) and a single electron only (right graph) at $T=100$ mK. The box-shaped symbols correspond to $B_\perp$, and the circles to $B_\parallel$. The singlet-triplet crossing in the two-electron system (due to the Zeeman splitting and the decrease of J) causes a jump in the magnetization around 5.5 T for $B_\parallel$, but no such signature occurs for $B_\perp$.

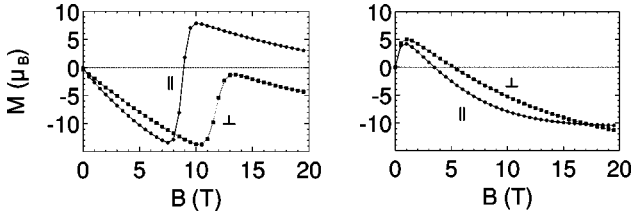

FIG. 7. Magnetization M (in units of Bohr magnetons) as a function of the B field for vertically coupled small InAs ($g=-15$) quantum dots (parameters as in Fig. 4) containing two electrons (left graph) and a single electron only (right graph) at $T=4$ K. The box-shaped symbols correspond to $B_\perp$, and the circles to $B_\parallel$. The singlet-triplet crossing in the two-electron system causes a jump in the magnetization around 9 T for $B_\parallel$, and one at about 12.5 T for $B_\perp$.

modified, since $\varphi_{\pm a}$ is not an exact eigenstate of the Hamiltonian $h^0_{\pm a}$ (cf. Appendix D). The correct expression for J in this case is

$$J(B,d)=J_0(B,d)-\hbar\omega_z\frac{4S^2}{1-S^4}\frac{\beta-\alpha}{\alpha}d^2\left(\frac{B}{B_0}\right)^2, \quad (21)$$

where J_0 denotes the expression from Eq. (9). The variation of the exchange energy J as a function of the magnetic field B is, through the prefactor $2S^2/(1-S^4)$, determined by the overlap $S(B,d)=\exp[-d^2(\beta(B)+(B/B_0)^2)/\alpha(B)]$, depending exponentially on the in-plane field, while for a perpendicular field the overlap is independent of the field (for two dots of equal size); see Eq. (11). We find that for weakly confined dots ($\hbar\omega_z\lesssim 10$ meV), there is a singlet-triplet crossing even without Zeeman interaction (J becoming negative as in Ref. 7); e.g., for $\hbar\omega_z=7$ meV, $\alpha_0=1/2$, and $2a=25$ nm we find such a singlet-triplet crossing at $B\approx 6$ T. Here we concentrate on more strongly confined dots ($\hbar\omega_z\gtrsim 10$ meV), where J remains positive for arbitrary B. Generally, the decay of J becomes flatter as the confinement is increased. Improving on the Heitler-London result, we again performed a molecular-orbital (Hund-Mulliken) calculation of the exchange energy, which we plot in Fig. 2 (left graph, circle symbols).

It is crucial in experiments to distinguish between single- and two-electron effects in the double dot, e.g., for potential quantum gate applications, where two electrons are required. A single electron in a double dot exhibits a level splitting of $2t$, where t denotes the single-particle tunneling matrix element [cf. Eq. (15)], which has a B field dependence similar to the exchange coupling J. In order to allow a distinction between J and t, we have plotted $t(B)$ in the right graph of Figs. 2 and 3. Since the one-particle tunneling matrix element t is strictly positive, it is clearly distinguishable from the exchange energy J in systems with singlet-triplet crossing. Experimentally, the number of electrons in the double-dot system can be tested via the field-dependent spectrum (Fig. 4) and magnetization (Figs. 6–8).

V. ELECTRICAL SWITCHING OF THE SPIN INTERACTION

Coupled quantum dots can potentially be used as quantum gates for quantum computation,[2,7] where the electronic spin on the dot plays the role of the qubit. Operating a coupled quantum dot as a quantum gate requires the ability to switch on and off the interaction between the electron spins on neighboring dots. Here we present a simple method of achieving a high-sensitivity switch for vertically coupled dots by means of a horizontally applied electric field $E_\parallel$. The idea is to use a pair of quantum dots with different lateral sizes, e.g., a small dot on top of a large dot ($\alpha_{0+}>\alpha_{0-}$; see Fig. 1). Note that only the radius in the xy plane has to be different, while we assume that the dots have the same height. Applying an in-plane electric field $E_\parallel$ in this case causes a shift of the single-dot orbitals by $\Delta x_\pm=eE_\parallel/m\omega_z^2\alpha_{0\pm}^2=E_\parallel/E_0\alpha_{0\pm}^2$, where $E_0=\hbar\omega_z/ea_B$; see Fig. 9. It is clear that the electron in the larger dot moves further in the (reversed) direction of the electric field ($\Delta x_->\Delta x_+$), since its confinement potential is weaker. As a result, the mean distance between the two electrons changes from $2d$ to $2d'$, where

$$d'=\sqrt{d^2+\frac{1}{4}(\Delta x_--\Delta x_+)^2}=\sqrt{d^2+A^2\left(\frac{E_\parallel}{E_0}\right)^2}, \quad (22)$$

with $A=(1/\alpha_{0-}^2-1/\alpha_{0+}^2)/2$. Using Eq. (11), we find that $S\propto\exp(-d'^2)\propto\exp[-A^2(E_\parallel/E_0)^2]$, i.e., the orbital overlap decreases exponentially as a function of the applied electric field $E_\parallel$. Due to this high sensitivity, the electric field is an

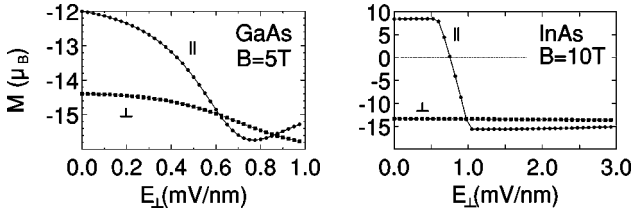

FIG. 8. Magnetization M (in units of Bohr magnetons) as a function of the perpendicular electric field $E_\perp$ for vertically coupled quantum dots containing two electrons at a fixed magnetic field. The box-shaped symbols correspond to $B_\perp$, and the circles to $B_\parallel$. Starting at $E=0$ with a triplet ground state for $B_\parallel$ (not so for $B_\perp$), the electric field eventually causes a change of the ground state back to the singlet, which leads again to a jump in the magnetization for $B_\parallel$. The left graph corresponds to a GaAs double dot (parameters as in Fig. 2) at $T=100$ mK and $B=5$ T, whereas the right graph is for a smaller InAs double dot (as in Fig. 3) at $T=4$ K and $B=10$ T.

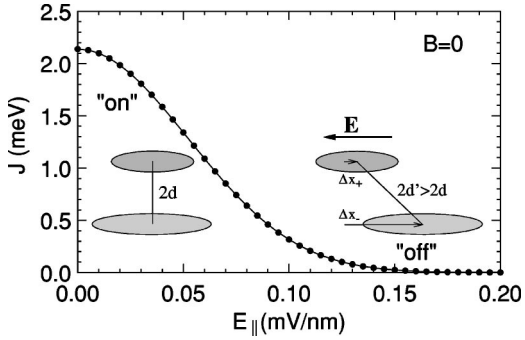

FIG. 9. Switching of the spin-spin coupling between dots of different size by means of an in-plane electric field $E_\parallel$ $(B=0)$. The exchange coupling is switched ''on'' at $E=0$. When an in-plane electric field $E_\parallel$ is applied, the larger of the two dots is shifted to the right by Δx_-, whereas the smaller dot is shifted by $\Delta x_+ < \Delta x_-$, where $\Delta x_\pm = E_\parallel / E_0 \alpha_{0\pm}^2$ and $E_0 = \hbar\omega_z / e a_B$. Therefore, the mean distance between the electrons in the two dots grows as $d' = \sqrt{d^2 + A^2 (E_\parallel / E_0)^2}$, where $A = (\alpha_{0+}^2 - \alpha_{0-}^2)/2\alpha_{0+}^2 \alpha_{0-}^2$. The exchange coupling J, being exponentially sensitive to the interdot distance d', thus decreases exponentially: $J \approx S^2 \approx \exp[-2A^2 (E_\parallel / E_0)^2]$. We have chosen $\hbar\omega_z = 7$ meV, $d=1$, $\alpha_{0+}=1/2$, and $\alpha_{0-}=1/4$. For these parameters, we find $E_0 = \hbar\omega_z / e a_B = 0.56$ mV/nm and $A = (\alpha_{0+}^2 - \alpha_{0-}^2)/2\alpha_{0+}^2 \alpha_{0-}^2 = 6$. The exchange coupling J decreases exponentially on the scale $E_0/2A = 0.047$ mV/nm for the electric field.

ideal ''switch'' for the exchange coupling J which is (asymptotically) proportional to S^2, and thus decreases exponentially on the scale $E_0/2A$. Note that if the dots have exactly the same size, then $A=0$ and the effect vanishes. We can obtain an estimate of J as a function of $E_\parallel$ by substituting d' from Eq. (22) into the Heitler-London result [Eq. (10)]. A plot of $J(E_\parallel)$ obtained in this way is shown in Fig. 9 for a specific choice of GaAs dots. Note that this procedure is not exact, since it neglects the tilt of the orbitals with respect to their connecting line. Exponential switching is highly desirable for quantum computation, because in the ''off'' state of the switch, fluctuations in the external control parameter (e.g., the electric field $E_\parallel$) or charge fluctuations cause only exponentially small fluctuations in the coupling J. If this were not the case, the fluctuations in J would lead to uncontrolled coupling between qubits and therefore to multiple-qubit errors. Such correlated errors cannot be corrected by known error-correction schemes, which are designed for uncorrelated errors.[36] It seems likely that our proposed switching method can be realized experimentally, e.g., in vertical columnar GaAs quantum dots,[16] with side gates controlling the lateral size and position of the dots, or in SAD's where one can expect different dot sizes in any case.

VI. SPIN MEASUREMENTS

The magnetization (Figs. 6–8), measured as an ensemble average over many pairs of coupled quantum dots in thermal equilibrium, reveals whether the ground-state of the coupled-dot system is a spin singlet or triplet. On the one hand, such a magnetization could be detected by a superconducting quantum interference device or with cantilever-based[37,38] magnetometers. This type of spin measurement was already suggested earlier for laterally coupled dots.[7] The distinction between a spin singlet $(S=0)$ and triplet $(S=1)$ is also possible using optical methods: Measurement of the Faraday rotation,[3,4] (caused by the precession of the magnetic moment around a magnetic field) reveals if the two-electron system is in a singlet $(S=0)$ with no Faraday rotation or in a triplet $(S=1)$ with finite Faraday rotation. Finally, it should also be possible to obtain spin information via optical (far-infrared) spectroscopy.[10]

We remark that if it is possible to measure the magnetization of just one individual pair of coupled dots, then this is equivalent to measuring a microscopic two spin-1/2 system, i.e., $1/2 \otimes 1/2 = 0 \oplus 1$. Elsewhere we described how such individual singlet and triplet states in a double dot can be detected (through their charge) in transport measurements via Aharonov-Bohm oscillations in the cotunneling current and/or current correlations.[39–41]

It is interesting to note that above scheme allows one to measure even a single spin 1/2, provided that, in addition, one can perform one two-qubit gate operation (corresponding to switching on the coupling J for some finite time) and a subsequent single-qubit gate by means of applying a local Zeeman interaction to one of the qubits. (Such local Zeeman interactions can be generated, e.g., by using local magnetic fields or by inhomogeneous g factors.[39]) Explicitly, such a single-spin measurement of the electron is performed as follows. We are given an arbitrary spin 1/2 state $|\alpha\rangle$ in quantum dot 1. For simplicity, we assume that $|\alpha\rangle$ is one of the basis states, $|\alpha\rangle = |\uparrow\rangle$ or $|\alpha\rangle = |\downarrow\rangle$; the generalization to a superposition of the basis states is straightforward. The spin in quantum dot 2 is prepared in the state $|\uparrow\rangle$. The interaction J between the spins in Eq. (1) is then switched on for a time τ_s, such that $\int_0^{\tau_s} J(t)dt = \pi/4$. By doing this, a ''square-root-of-swap'' gate[2,34] is performed for the two spins (qubits). In the case $|\alpha\rangle = |\uparrow\rangle$, nothing happens, i.e., the spins remain in the state $|\uparrow\uparrow\rangle$, whereas, if $|\alpha\rangle = |\downarrow\rangle$, then we obtain the entangled state $(|\downarrow\uparrow\rangle + i|\uparrow\downarrow\rangle)/\sqrt{2}$, (up to a phase factor which can be ignored). Finally, we apply a local Zeeman term $g\mu_B B S_z^1$, acting parallel to the z axis at quantum dot 1 during the time interval τ_B, such that $\int_0^{\tau_B} (g\mu_B B)(t)dt = \pi/2$. The resulting state is (again up to unimportant phase factors) the triplet state $|\uparrow\uparrow\rangle$ in the case where $|\alpha\rangle = |\uparrow\rangle$, whereas we obtain the singlet state $(|\uparrow\downarrow\rangle - |\downarrow\uparrow\rangle)/\sqrt{2}$ in the case $|\alpha\rangle = |\downarrow\rangle$. In other words, such a procedure maps the triplet $|\uparrow\uparrow\rangle$ into itself and the state $|\downarrow\uparrow\rangle$ into the singlet [similarly, the same gate operations map $|\downarrow\downarrow\rangle$ into itself, while $|\uparrow\downarrow\rangle$ is mapped into the triplet $(|\uparrow\downarrow\rangle + |\downarrow\uparrow\rangle)/\sqrt{2}$, again up to phase factors]. Finally, measuring the total magnetic moment of the double dot system then reveals which of the two spin states in dot 1, $|\uparrow\rangle$ or $|\downarrow\rangle$, was realized initially.

VII. DISCUSSION

In summary, we have calculated the spin exchange interaction $J(\mathbf{B},\mathbf{E})$ for electrons confined in a pair of vertically coupled quantum dots, and have compared the two-electron spectra (with level splitting J) to the single-electron spectra (with level splitting $2t$). Comparing the one- and two-electron spectra enables us to distinguish one-electron filling from two-electron filling of the double dot in an experiment. For two-electron filling in the presence of a magnetic field, a

ground-state crossing from a singlet to a triplet occurs at fields of about 5–10 T, depending on the strength of the confinement, the coupling, and the effective g factor. The crossing can be reversed by applying a perpendicular electric field.

As a model for the electron confinement in a quantum dot, we have chosen harmonic potentials. However, in some situations (especially self-assembled quantum dots) it is more accurate to use square-well confinement potentials in order to model the band-gap offset between different materials. We have also performed calculations using square-well potentials, which confirm the qualitative behavior of the results obtained using harmonic potentials. The results from using the square-well model potentials cannot be written in simple algebraic expressions, and are given elsewhere.[33]

Furthermore, we have analyzed the possibilities of switching the spin-spin interaction J using external parameters. We find that in-plane magnetic fields $B_{\|}$ (perpendicular to the interdot axis) are better suited for tuning the exchange coupling in a vertical double-dot structure than a field $B_{\perp}$ (applied along the interdot axis). Moreover, we have confirmed that the dependence of the exchange energy on a magnetic field is stronger for weakly confined dots than for structures with strong confinement. An even more efficient switching mechanism is found when a small quantum dot is coupled to a large dot: In this case, the coupling J depends exponentially on the in-plane electric field $E_{\|}$, and thus provides an ideal external parameter for switching the spin coupling on and off with exponential sensitivity. The experimental confirmation of the electrical switching effect would be an important step toward solid-state quantum computation with quantum dots.

Another (very demanding) key experiment for quantum computation in quantum dots is the measurement of single-electron spins. Here we have presented a theoretical scheme for a single-spin measurement using coupled quantum dots. Obviously this scheme already requires some controlled interaction between the spins (qubits), and therefore the successful implementation of some switching mechanisms.

ACKNOWLEDGMENTS

We would like to thank D.D. Awschalom, D.P. DiVincenzo, R.H. Blick, P.M. Petroff, and E.V. Sukhorukov for useful discussions. This work was supported by the Swiss National Science Foundation.

APPENDIX A: HUND-MULLIKEN MATRIX ELEMENTS

Here we list the explicit expressions for the matrix elements defined in Eqs. (13)–(17) for two dots with arbitrary (and possibly different) single-electron Hamiltonians $h_{\pm a}$ and (nonorthogonal) single-electron orbitals $\varphi_{\pm a}$ centered at $z=\pm a$. The matrix elements are

$$V_+ = N^4[2g^2(G_1^+ + G_1^-) + 4g^2S^2G_1^0 + 4g^2G_2 + (1+g^2)^2G_3 - 6g^2(G_4^+ + G_4^-)], \tag{A1}$$

$$V_- = N^4(1-g^2)^2[G_3 - S^2G_2], \tag{A2}$$

$$U_\pm = N^4[G_1^\pm + g^4G_1^\mp + 2g^2S^2G_1^0 + 2g^2S^2(G_2+G_3) - 4gS(G_4^\pm - g^2G_4^\mp)], \tag{A3}$$

$$X = N^4[(1+g^4)S^2G_1^0 + g^2(G_1^+ + G_1^-) + 2g^2S^2G_2 + 2g^2G_3 - 2g(1+g^2)S(G_4^+ + G_4^-)], \tag{A4}$$

$$w_\pm = N^4[-gG_1^\pm - g^3G_1^\mp - g(1+g^2)(2S^2G_1^0 + G_3) + S(1+3g^2)G_4^\pm + S^2g^2(1+g^2)G_4^\mp], \tag{A5}$$

with $N = 1/\sqrt{1-2Sg+g^2}$ and $g = (1-\sqrt{1-S^2})/S$. We have introduced the overlap integrals

$$G_1^\pm = \langle \varphi_{\pm a}\varphi_{\pm a}|C|\varphi_{\pm a}\varphi_{\pm a}\rangle, \tag{A6}$$

$$G_1^0 = S^{-2}\langle \varphi_{\pm a}\varphi_{\pm a}|C|\varphi_{\mp a}\varphi_{\mp a}\rangle, \tag{A7}$$

$$G_2 = S^{-2}\langle \varphi_{\pm a}\varphi_{\mp a}|C|\varphi_{\mp a}\varphi_{\pm a}\rangle, \tag{A8}$$

$$G_3 = \langle \varphi_{\pm a}\varphi_{\mp a}|C|\varphi_{\pm a}\varphi_{\mp a}\rangle, \tag{A9}$$

$$G_4^\pm = S^{-1}\langle \varphi_{\pm a}\varphi_{\pm a}|C|\varphi_{\pm a}\varphi_{\mp a}\rangle. \tag{A10}$$

Note that the expressions for G_1^0, G_2, and G_3 are invariant under exchange of φ_a and φ_{-a}. In the case where the two single-particle Hamiltonians coincide (implying that the dots have the same size), we find $G_1^+ = G_1^-$ $(= G_1^0$, since C depends only on the relative coordinate) and $G_4^+ = G_4^-$, and the expressions in Eqs. (A1)–(A5) for the matrix elements can be simplified accordingly. This simplification leads to the same form of the Hund-Mulliken matrix elements which we have calculated for laterally coupled dots.[7] If it is possible to choose the orbitals $\varphi_{\pm a}$ to be real; e.g., if the magnetic field is in the z direction, then $G_1^0 = G_2$, leading to a further simplification of the matrix elements [Eqs. (A1)–(A5)].

APPENDIX B: HUND-MULLIKEN MATRIX ELEMENTS, $B \perp x,y$

If the single-electron Hamiltonian is given by Eq. (5) with a perpendicular field $B \perp x,y$ then we can further evaluate the integrals Eqs. (A6)–(A10) and the single-particle matrix elements in Eqs. (13)–(17) as a function of the dimensionless interdot distance $d = a/a_B$ and the magnetic compression factors $\alpha_\pm(B) = \sqrt{\alpha_{0\pm}^2 + B^2/B_0^2}$. The single-particle matrix elements are given by

$$\epsilon_\pm = \frac{\hbar\omega_z}{2}\left\{1 + \frac{3}{16d^2} + \frac{S}{1-S^2}\left[\frac{\alpha_\pm}{g} + g\alpha_\mp \pm \frac{1}{4}\frac{\alpha_{0+}^2 - \alpha_{0-}^2}{\alpha_+\alpha_-}\left(g\alpha_\pm - \frac{\alpha_\mp}{g}\right)[1-\mathrm{erf}(d)]\right] + \frac{S^2}{1-S^2}\left(\frac{3}{4}(1+d^2) - (\alpha_\pm + \alpha_\mp)\right)\right\}, \tag{B1}$$

$$t=\frac{\hbar\omega_z}{2}\frac{S}{1-S^2}\left[\frac{1}{4}\frac{\alpha_{0+}^2-\alpha_{0-}^2}{\alpha_+\alpha_-}[1-\mathrm{erf}(d)](\alpha_+-\alpha_-)+\frac{3}{4}(1+d^2)\right], \tag{B2}$$

where $S=[2\sqrt{\alpha_+\alpha_-}/(\alpha_++\alpha_-)]\exp(-d^2)$. The (two-particle) Coulomb matrix elements can be expressed as in Eqs. (A1)–(A5), where the integrals [Eqs. (A6)–(A10)] take the forms

$$G_1^{\pm}=\hbar\omega_z\frac{2c}{\pi}\frac{\alpha_\pm}{\sqrt{1-(2\alpha_\pm-1)^2}}\arccos(2\alpha_\pm-1), \tag{B3}$$

$$G_2=G_1^0=\hbar\omega_z\frac{c}{\pi}\frac{\alpha_++\alpha_-}{\sqrt{1-(\alpha_++\alpha_--1)^2}}\arccos(\alpha_++\alpha_--1), \tag{B4}$$

$$G_3=\hbar\omega_z\sqrt{\mu}c\,\exp(2\mu d^2)[1-\mathrm{erf}(d\sqrt{2\mu})], \tag{B5}$$

$$G_4^{\pm}=\hbar\omega_z c\sqrt{\frac{2\alpha_\pm(\alpha_++\alpha_-)}{3\alpha_++\alpha_-}}\exp(\mu_\pm d^2)[1-\mathrm{erf}(d\sqrt{\mu_\pm})], \tag{B6}$$

where we have introduced $\mu=2\alpha_+\alpha_-/(\alpha_++\alpha_-)$ and $\mu_\pm=(\alpha_\pm^2+\alpha_+\alpha_-)/(3\alpha_\pm+\alpha_\mp)$. Equations (B5) and (B6) are approximations which deviate from the exact result by $<12\%$ in the range $d>0.7$ and $\mu\leqslant 1$, as we have checked by numerical evaluation of the integrals.

APPENDIX C: HUND-MULLIKEN MATRIX ELEMENTS, $B\|x$

The Hund-Mulliken calculation for a system of two equal dots with a magnetic field applied in the x direction (Sec. IV) is formally identical to the one with a field in the z direction presented in Sec. III. For equal dots we set $\alpha_{0+}=\alpha_{0-}\equiv\alpha_0$, $\alpha_+=\alpha_-\equiv\alpha$, and $\epsilon_+=\epsilon_-\equiv\epsilon$. The one-particle matrix elements are then

$$\epsilon=\frac{\hbar\omega_z}{2}\left[\alpha_0+\alpha+\beta+\frac{3}{16d^2\beta^2}+\frac{S^2}{1-S^2}\frac{3}{4}\left(\frac{1}{\beta}+d^2\right)-\frac{S^2}{1-S^2}\frac{\beta-\alpha}{\alpha}2d^2\left(\frac{B}{B_0}\right)^2\right], \tag{C1}$$

$$t=\frac{\hbar\omega_z}{2}\frac{S}{1-S^2}\left[\frac{3}{4}\left(\frac{1}{\beta}+d^2\right)-\frac{\beta-\alpha}{\alpha}2d^2\left(\frac{B}{B_0}\right)^2\right]. \tag{C2}$$

Since we consider two equal dots, the matrix elements of the Coulomb Hamiltonian are formally equal to those given in Ref. 7, where F_i has to be replaced by G_i, defined by

$$G_1\equiv G_1^+=G_1^-=G_1^0=\hbar\omega_z\frac{c}{\pi}\sqrt{\alpha\alpha_0\beta}\int_0^\infty dr\,rK_0\left(\frac{\beta r^2}{4}\right)\mathrm{I}_0\left(\frac{\alpha-\alpha_0}{4}r^2\right)\times e^{-(1/4)(\alpha+\alpha_0-\beta)r^2}, \tag{C3}$$

$$G_2=\hbar\omega_z\frac{c}{\pi}\sqrt{\alpha\alpha_0\beta}\int_0^\infty dr\int_{-\infty}^\infty dz\,\frac{r}{\sqrt{r^2+z^2}}I_0\left(\frac{\alpha-\alpha_0}{4}r^2\right)\times e^{-(1/4)(\alpha+\alpha_0)r^2-(1/2)\beta(z+2d)^2}, \tag{C4}$$

$$G_3=\hbar\omega_z\frac{c}{\pi}\sqrt{\alpha\alpha_0\beta}e^{d^2(B/B_0)^2/\alpha}\int_0^\infty dr\int_{-\infty}^\infty dy\,\frac{r}{\sqrt{r^2+y^2}}\times\mathrm{I}_0\left(\frac{\beta-\alpha_0}{4}r^2\right)e^{-(1/4)(\beta+\alpha_0)r^2-(1/2)\alpha y^2}\times\cos(2ydB/B_0), \tag{C5}$$

$$G_4\equiv G_4^+=G_4^-=\hbar\omega_z\frac{c}{2\pi^2}\sqrt{\alpha\alpha_0\beta}\int_{-\infty}^\infty dy\int_{-\infty}^\infty dz K_0\left(\frac{\alpha_0}{4}(y^2+z^2)\right)e^{-(1/4)(2\alpha-\alpha_0)y^2-(1/2)\beta(z-d)^2+\frac{1}{4}\alpha_0 z^2}\cos(ydB/B_0). \tag{C6}$$

Here K_0 denotes the zeroth-order Macdonald function, and I_0 is the zeroth-order modified Bessel function. The quantities α, β, and S have been defined earlier.

APPENDIX D: HEITLER-LONDON CALCULATIONS, $B\|x$

In the following we evaluate the exchange energy J for two coupled quantum dots in a magnetic field applied perpendicularly to the interdot axis ($\mathbf{B}\|\mathbf{x}$) using the Heitler-London approach. We first study the one-particle problem for an anisotropic quantum dot with a magnetic field applied perpendicularly to the symmetry axis of the dot,

$$h^0(\mathbf{r})=\frac{1}{2m}\left(\mathbf{p}-\frac{e}{c}\mathbf{A}(\mathbf{r})\right)^2+\frac{m\omega_z^2}{2}[\alpha_0^2(x^2+y^2)+z^2], \tag{D1}$$

where α_0 is the ellipticity and $\mathbf{A}(\mathbf{r})=B(0,-z,y)/2$. We can separate $h^0(\mathbf{r})=h_x^0(x)+h_{yz}^0(y,z)$ into a B-independent harmonic oscillator $h_x^0(x)=-(\hbar^2/2m)\partial_x^2+(m\omega_z^2/2)\alpha_0^2x^2$, and a B-dependent part

$$h_{yz}^0(y,z)=p_y^2+p_z^2-\omega_L L_x+\frac{m_z\omega^2}{2}(\alpha^2y^2+\beta^2z^2), \tag{D2}$$

with $\alpha=\sqrt{\alpha_0^2+(\omega_L/\omega_z)^2}=\sqrt{\alpha_0^2+(B/B_0)^2}$, and $\beta=\sqrt{1+(\omega_L/\omega_z)^2}=\sqrt{1+(B/B_0)^2}$. We have not solved Eq. (D2) exactly; instead we have used a variational approach, minimizing the single-particle energy $\epsilon_0=\langle\psi|h_{yz}^0|\psi\rangle/\langle\psi|\psi\rangle$ as a function of two variational parameters, in order to find a good approximate ground-state wave function. A reasonable trial wave function ψ should reproduce the anisotropy between y and z in the Hamiltonian. This requirement is ful-

filled, e.g., by a Gaussian $\psi_1(\gamma_1,\gamma_2,y,z)=\mathcal{N}e^{-\gamma_1 y^2-\gamma_2 z^2}$, or by mixing Fock-Darwin states $\psi_{0,l}$ with angular momenta $l=0$, 2, and -2 and radial quantum number $n=0$, $\psi_2(\delta_2,\delta_{-2},y,z)=\tilde{\mathcal{N}}[\psi_{0,0}(y,z)+\Sigma_{l=\pm 2}\delta_l\psi_{0,l}(y,z)]$, where δ_{-2},δ_2, and γ_1,γ_2 are variational parameters and $\mathcal{N}$ and $\tilde{\mathcal{N}}$ are normalization constants. Calculating $\epsilon_0(\gamma_1,\gamma_2)$ and $\epsilon_0(\delta_{-2},\delta_2)$, and subsequently minimizing with respect to the variational parameters, we find that $\psi_1[m\omega_z\alpha/(2\hbar),m\omega_z\beta/(2\hbar),y,z]$, with the normalization constant $\mathcal{N}=(m\omega_z/\pi\hbar)^{1/2}(\alpha\beta)^{1/4}$, is the best approximate ground-state wave function in our variational space. We have also shown that including the Fock-Darwin states with angular momentum quantum numbers $l=\pm 1$ in ψ_2 does not lead to a lower minimum of the energy $\langle\psi_2|h^0_{yz}|\psi_2\rangle/\langle\psi_2|\psi_2\rangle$. The full one-particle wave function is then given by

$$\varphi(x,y,z)=\left(\frac{m\omega_z}{\pi\hbar}\right)^{3/4}(\alpha_0\alpha\beta)^{1/4}e^{-m\omega_z(\alpha_0x^2+\alpha y^2+\beta z^2)/2\hbar}. \tag{D3}$$

Shifting the single-particle orbitals to $(0,0,\pm a)$ in the presence of a magnetic field, we obtain Eq. (20), where the phase factor involving the magnetic length $l_B=\sqrt{\hbar c/eB}$ is due to the gauge transformation $\mathbf{A}_{\pm a}=B(0,-[z\mp a],y)/2\rightarrow\mathbf{A}=B(0,-z,y)/2$. Having found an approximate solution for the one-particle problem in a dot centered at $z=+a$ or $z=-a$, we show that the exchange energy is given by Eq. (21) for a system with two dots of equal size, where J_0 denotes the result from Eq. (9). In the derivation of the formal expression for the exchange energy $J_0(B,d)$ given in Eq. (9), we have used that $\varphi_{\pm a}$ was an exact eigenstate of $h^0_{\pm a}$, and therefore $\langle\varphi_{\mp a}|h^0_{\pm a}|\varphi_{\pm a}\rangle=S\langle\varphi_{\pm a}|h^0_{\pm a}|\varphi_{\pm a}\rangle$, where $S=\langle\varphi_a|\varphi_{-a}\rangle$ denotes the overlap of the shifted orbitals. The approximate solution [Eq. (D3)] for an anisotropic dot in the presence of an in-plane magnetic field is not an exact eigenstate of h^0. Using the corrected off-diagonal matrix element $\langle\varphi_{\mp a}|h^0_{\pm a}|\varphi_{\pm a}\rangle=S[\hbar\omega_z(\alpha_0+\alpha+\beta)/2+d^2(B/B_0)^2(\beta-\alpha)/\alpha]$, the result for the exchange energy [Eq. (21)] can easily be derived.

*Electronic address: guido.burkard@unibas.ch
†Electronic address: daniel.loss@unibas.ch

[1] G.A. Prinz, Phys. Today **48**(4), 58 (1995); Science **282**, 1660 (1998).
[2] D. Loss and D. P. DiVincenzo, Phys. Rev. A **57**, 120 (1998).
[3] J.M. Kikkawa and D.D. Awschalom, Phys. Rev. Lett. **80**, 4313 (1998).
[4] J.A. Gupta, D.D. Awschalomk, X. Peng, and A.P. Alivisatos, Phys. Rev. B **59**, 10 421 (1999).
[5] P.W. Shor, in *Proceedings of the 35th Annual Symposium on the Foundations of Computer Science* (IEEE Press, Los Alamitos, CA, 1994), p. 124.
[6] L.K. Grover, Phys. Rev. Lett. **79**, 325 (1997).
[7] G. Burkard, D. Loss, and D.P. DiVincenzo, Phys. Rev. B **59**, 2070 (1999).
[8] M.A. Kastner, Phys. Today **46**(1), 24 (1993); R.C. Ashoori, Nature (London) **379**, 413 (1996).
[9] L.P. Kouwenhoven, C. M. Marcus, P. L. McEuen, S. Tarucha, R. M. Westervelt, and N. S. Wingreen, in *Proceedings of the Advanced Study Institute on Mesoscopic Electron Transport*, edited by L. L. Sohn, L.P. Kouwenhoven, and G. Schön (Kluwer, Dordrecht, 1997).
[10] L. Jacak, P. Hawrylak, and A. Wójs, *Quantum Dots* (Springer, Berlin, 1997).
[11] S. Tarucha, D.G. Austing, T. Honda, R.J. van der Hage, and L.P. Kouwenhoven, Phys. Rev. Lett. **77**, 3613 (1996); L.P. Kouwenhoven, T. H. Oosterkamp, M. W. S. Danoesastro, M. Eto, D. G. Austing, T. Honda, and S. Tarucha, Science **278**, 1788 (1997).
[12] F.R. Waugh, M. J. Berry, D. J. Mar, R. M. Westervelt, K. L. Chapman, and A. C. Gossard, Phys. Rev. Lett. **75**, 705 (1995).
[13] C. Livermore, C.H. Crouch, R.M. Westervelt, K.L. Chapman, and A.C. Gossard, Science **274**, 1332 (1996).
[14] R.H. Blick, R. J. Haug, J. Weis, D. Pfannkuche, K. v. Klitzing, and K. Eberl, Phys. Rev. B **53**, 7899 (1996); R.H. Blick, D. Pfannkuche, R.J. Haug, K. von Klitzing, and K. Eberl, Phys. Rev. Lett. **80**, 4032 (1998); R.H. Blick, D.W. van der Weide, R.J. Haug, and K. Eberl, *ibid.* **81**, 689 (1998).
[15] T.H. Oosterkamp, T. Fujisawa, W. G. van der Wiel, K. Ishibashi, R. V. Hijman, S. Tarucha, and L. P. Kouwenhoven, Nature **395**, 873 (1998).
[16] D. G. Austing, T. Honda, K. Muraki, Y. Tokura, and S. Tarucha, Physica B **249-251**, 206 (1998).
[17] S. Fafard, Z. R. Wasilewski, C. Ni Allen, D. Picard, M. Spanner, J. P. McCaffrey, and P. G. Piva, Phys. Rev. B **59**, 15 368 (1999).
[18] R.J. Luyken, A. Lorke, M. Haslinger, B. T. Miller, M. Fricke, J. P. Kotthaus, G. Medeiros-Ribiero, and P. M. Petroff (unpublished).
[19] M. Fricke, A. Lorke, J.P. Kotthaus, G. Medeiros-Ribeiro, and P.M. Petroff, Europhys. Lett. **36**, 197 (1996).
[20] L. Goldstein, F. Glas, J.Y. Marzin, M.N. Charasse, and G. Le Roux, Appl. Phys. Lett. **47**, 1099 (1985); D. Leonard, M. Krishnamurthy, C.M. Reaves, S.P. Denbaars, and P.M. Petroff, *ibid.* **63**, 3203 (1993); J.-Y. Marzin, J.-M. Gérard, A. Izraël, D. Barrier, and G. Bastard, Phys. Rev. Lett. **73**, 716 (1994); H. Drexler, D. Leonard, W. Hansen, J.P. Kotthaus, and P.M. Petroff, *ibid.* **73**, 2252 (1994); M. Grundmann *et al.*, *ibid.* **74**, 4043 (1995).
[21] Q. Xie, A. Madhukar, P. Chen, and N.P. Kobayashi, Phys. Rev. Lett. **75**, 2542 (1995); J. Tersoff, C. Teichert, and M.G. Lagally, *ibid.* **76**, 1675 (1996).
[22] J.J. Palacios and P. Hawrylak, Phys. Rev. B **51**, 1769 (1995).
[23] S.C. Benjamin and N.F. Johnson, Phys. Rev. B **51**, 14 733 (1995).
[24] B. Partoens, A. Matulis, and F. M. Peeters, Phys. Rev. B **59**, 1617 (1999).
[25] G.W. Bryant, Phys. Rev. B **48**, 8024 (1993).
[26] M. Wagner, U. Merkt, and A.V. Chaplik, Phys. Rev. B **45**, 1951 (1992); A. Wojs, P. Hawrylak, S. Fafard, and L. Jacak, *ibid.* **54**, 5604 (1996).
[27] J.H. Oh, K.J. Chang, G. Ihm, and S.J. Lee, Phys. Rev. B **53**, R13 264 (1996).
[28] H. Imamura, P.A. Maksym, and H. Aoki, Phys. Rev. B **53**, 12 613 (1996); H. Imamura, H. Aoki, and P.A. Maksym, *ibid.* **57**, R4257 (1998); H. Imamura, P.A. Maksym, and H. Aoki, *ibid.* **59**, 5817 (1999).
[29] Y. Tokura, D.G. Austing, and S. Tarucha, J. Phys. C **11**, 6023 (1999).
[30] T.H. Oosterkamp, S. F. Godijn, M. J. Uilenreef, Y. V. Nazarov,

N. C. van der Vaart, and L. P. Kouwenhoven, Phys. Rev. Lett. **80**, 4951 (1998).

[31] A. Wojs, P. Hawrylak, S. Fafard, and L. Jacak, Phys. Rev. B **54**, 5604 (1996).

[32] V. Fock, Z. Phys. **47**, 446 (1928); C. Darwin, Proc. Cambridge Philos. Soc. **27**, 86 (1930).

[33] G. Seelig, Diploma thesis, University of Basel, 1999.

[34] G. Burkard, D. Loss, D.P. DiVincenzo, and J.A. Smolin, Phys. Rev. B **60**, 11 404 (1999).

[35] For $\hbar\omega_z \approx 20$ meV and $\alpha_{0\pm} = 1/2$ the approximation is about 5% off at $B=0$, while for $B=B_0 \approx 20$ T the approximation deviates about 12% from the exact value.

[36] J. Preskill, Proc. R. Soc. London Ser. A **454**, 385 (1998).

[37] K. Wago, D. Botkin, C.S. Yannoni, and D. Rugar, Phys. Rev. B **57**, 1108 (1998).

[38] J.G.E. Harris, D. D. Awschalom, F. Matsukura, H. Ohno, K. D. Maranowski, and A. C. Gossard, Appl. Phys. Lett. **75**, 1140 (1999).

[39] D.P. DiVincenzo and D. Loss, J. Magn. Magn. Mater. **200**, 202 (1999) [cond-mat/9901137].

[40] G. Burkard, D. Loss, and E.V. Sukhorukov, Phys. Rev. B (to be published).

[41] D. Loss and E.V. Sukhorukov, Phys. Rev. Lett. **84**, 1035 (2000).